UTC(OP) based on LNE-SYRTE atomic fountain primary frequency standards

Daniele Rovera, S. Bize, B. Chupin, J. Guena, Ph Laurent, P. Rosenbusch, P. Uhrich, Michel Abgrall

HAL Id: obspm-02319605

https://hal-obspm.ccsd.cnrs.fr/obspm-02319605

Submitted on 10 Sep 2021

UTC(OP) based on LNE-SYRTE atomic fountain primary frequency standards

To cite this article: G D Rovera *et al* 2016 *Metrologia* **53** S81

View the article online for updates and enhancements.

UTC(OP) based on LNE-SYRTE atomic fountain primary frequency standards

G D Rovera, S Bize, B Chupin, J Guéna, Ph Laurent, P Rosenbusch, P Uhrich and M Abgrall

LNE-SYRTE, Observatoire de Paris, PSL Research University, CNRS, Sorbonne Universités, UPMC University Paris 06, 61 avenue de l'Observatoire, 75014 Paris, France

E-mail: daniele.rovera@obspm.fr

CrossMark

Abstract

UTC(OP), the French national realization of the international coordinated universal time, was redesigned and rebuilt. The first step was the implementation in October 2012 of a new algorithm based on a H-maser and on atomic fountain data. Thanks to the new implementation, the stability of UTC(OP) was dramatically improved and UTC(OP) competes with the best time scales available today. Then the hardware generation and distribution of the UTC(OP) physical signals were replaced. Part of the new hardware is composed of commercial devices, but the key elements were specifically developed. One of them is a special switch that allows the UTC(OP) signals to be derived from one of two time scales, based on two different H-masers, which are generated simultaneously. This insures the continuity of the UTC(OP) signal even when a change of the reference H-maser is required. With the new hardware implementation, UTC(OP) is made available through three coherent signals: 100 MHz, 10 MHz and 1 PPS. For more than 3 years, UTC(OP) remained well below 10 ns close to UTC, with a difference even less than 5 ns if we except a short period around MJD 56650.

Keywords: UTC(k), stability, primary frequency standard, time scale algorithm

(Some figures may appear in colour only in the online journal)

1. Introduction

By definition, the real-time realization of the coordinated universal time (UTC) by a laboratory k is called UTC(k). The legal time of a country is generally based on the UTC(k) generated by its National Metrology Institute (NMI), or by a designated laboratory like LNE-SYRTE in Observatoire de Paris (OP) is for France. There are no stringent technical requirements for a UTC(k). In 1993 the Comité Consultatif pour la Définition de la Seconde (CCDS) recommended: *'that time centres provide information to facilitate time coordination to UTC in real time with a goal of 100 ns, standard deviation, when this is feasible'* [1]. In practice this recommendation is fulfilled by more than two thirds of the seventy laboratories generating a UTC(k). A UTC(k) stable enough and close to UTC might be an indicator of the metrological capability of a laboratory. However, this is the case only when the laboratory can demonstrate that the UTC(k) is realized in an independent way. Here 'independent' means that the only inputs are some local clock data plus the *Circular T* for the steering to UTC.

For many years UTC(OP) was realized by steering the output signal of a commercial Cs beam frequency standard, the amount of the correction being evaluated heuristically [2]. By 29 October, 2012, (MJD 56229) a new realization of UTC(OP) based on the steering of an active H-maser, driven by the LNE-SYRTE atomic fountains by using a frequency offset generator, was implemented. A description of the algorithm and of the underlying philosophy is given in section 2, followed by an exhaustive description of the hardware in section 3. The results obtained in the first three years of operation are reported in section 4.

2. UTC(OP) algorithm

The CCDS recommendation of 1993 [1] only indicates the limits of the deviation between a UTC(k) and UTC, but does not put any other constraint on a UTC(k) generation. As a consequence there are many interpretations of what the goal in the implementation of a UTC(k) is. In some cases the design of the algorithm privileges the stability of the time interval (i.e. frequency), while accepting relatively large deviations from UTC [3]. In the case of UTC(OP) the goal is to generate a physical signal, available in real time, which best represents UTC, by considering that UTC is only available with a latency that can reach 40 d. The algorithm developed for this purpose is based on two assumptions:

- UTC is the most stable time scale available.
- we can generate a time scale with a stability comparable to the UTC one.

It is obvious that the deviation between UTC(OP) and UTC will be limited by the stability of both time scales. Any irregularity of one of them will be observed with a one month delay and therefore there is no way to forecast a correction for that event.

Based on these considerations, two steps can be easily identified in the generation of a UTC(k):

- first, to implement a time scale with a time interval duration exhibiting the best achievable stability, regardless of the time interval duration.
- second, to implement a frequency/phase lock loop to adjust the duration of the time interval to UTC and to reduce the time deviation to a minimum value, by taking into account the stability of the loop.

The algorithm can therefore be designed as two separate blocks. In the specific case of UTC(OP), the two blocks will share the same actuator, but they are conceptually well distinct. Even if the frequency of a good H-maser is highly predictable, we take advantage of our ensemble of atomic fountains, developed by LNE-SYRTE as primary and secondary frequency standard (PSFS) [4–8], to accurately evaluate the frequency of the H-maser used for the realization of UTC(OP). The algorithm is based on a single H-maser measured almost continuously against a single fountain. However, as explained in section 3 the actually used H-maser, or fountain, can easily be replaced by another one at any time.

The first block of the algorithm can be described as a special type of feed-forward open loop control. It provides the main part of the H-maser frequency correction which is of the order of several 10^{-13}. The concern in developing this part was to privilege the robustness, without searching for the best stability performances because the most important feature of a UTC(k) time scale is the continuity of operation. By considering the stability of the chosen H-maser and fountain, we update the frequency correction applied to the frequency offset generator once a day. But to take advantage of the long term stability of the H-maser and to obtain a system robust against fountain missing data, the frequency of the H-maser is evaluated by a linear fit over the last 20 d, extrapolated to the

time of the application of the correction. In this way, even in the case of a few days of missing data due to possible problems in signal distribution, in fountain operation or in data processing, the frequency of the H-maser is estimated within an uncertainty well below 10^{-15}. A shorter integration period would probably increase the stability because it would control more tightly the frequency of the H-maser. But in this case a few days of missing fountain data would have a large impact. At this first step the correction will generate a signal that realizes the definition of the SI second.

By using the free running H-maser as the local oscillator of the fountain, and by applying the correction in a feed-forward way, we get rid of the drawbacks of the closed loop techniques, notably of the in-loop oscillations. Although a rigorous analysis of the noise of this system is beyond the scope of this paper, we can reasonably infer that the output noise is a replica of the free-running H-maser noise for periods of 1 d and shorter, then slowly converging to the noise of the fountain for integration times of 10 d or more.

The underlying concept of this control loop is the use of time series of data, sampled at a time shorter than the loop sampling time, and extrapolated, after outliers removal, to the epoch at which the correction is effectively applied. This concept was previously tested in a totally different context to lock the frequency of a quartz oscillator to the frequency of a 633 nm HeNe laser stabilized on an I_2 absorption line [9].

The second block of the algorithm is a closed loop control system. It provides a fine steering updated monthly, typically of the order of 10^{-15}, allowing for UTC(OP) to remain close to UTC. The control loop has to cope with the delay of UTC data availability. The *Circular T* is indeed published only monthly, and there is a delay of about 10 d between the end of the monthly period and the effective release of the data. The data are the differences UTC(k)–UTC every 5 d (MJD ending by 4 or 9) of the given month. The simplest approach can be the classical phase locked loop (PLL), where the input variable is the phase (time in this case) difference between UTC and UTC(OP), and the control variable is the frequency correction introduced by the frequency offset generator. This configuration benefits of a true integrator, because of the relationship between phase and frequency. However the stability rules [10] impose that for a PLL the gain must be well below unity at a frequency reciprocal of the time delay. The chosen solution is a combination of a frequency locked loop (FLL) and of a PLL.

The FLL consists in the evaluation of the difference of frequency between UTC and UTC(OP) during the period covered by the last available *Circular T*. The resulting value gives the first part of the monthly steering that is kept constant up to the next *Circular T* release. This constitutes a first order loop with unity gain at the one month sampling period of the system. There is thus no risk of oscillation.

For the PLL part, the time difference at the time of the publication of the *Circular T* is estimated by extrapolating the *Circular T* data. The contribution of the PLL to the frequency correction is then evaluated by dividing the time difference by 60 d. The extrapolation in some way allows to get rid of the *Circular T* release delay, and the low gain of 0.5
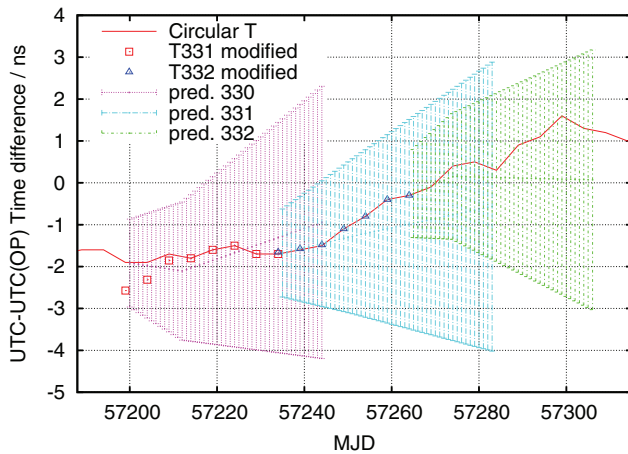
Figure 1. UTC–UTC(OP) differences. Data extracted from the *Circular T* (one point at MJD ending by 4 or 9), and prediction of UTC–UTC(OP) (one point per day). The explanations are given in the text.

at the loop sampling period does not allow for gain induced oscillations.

The goal is to obtain the best estimation of the frequency over the last published *Circular T* interval together with the expected phase difference with the current correction applied. For the evaluation of the frequency difference between UTC and UTC(OP), it must be taken into account that the previous correction had been applied at about one third of the last one month observation period. Therefore the first UTC–UTC(OP) deviations provided by the last published *Circular T* have to be modified by taking into account the difference between the current steering coefficient and the previous one. This operation is put in evidence by the empty red squares in figure 1 which gives the example of the steering applied after the release of *Circular T* 330 at MJD 57212. In this graph the squares are superposed to the red line that represents UTC–UTC(OP) as published in *Circular T*. But for epochs preceding MJD 57212, a correction coefficient different by 6.04×10^{-16} from the current one, corresponding to the steering of the previous month, was already applied. Hence the points prior to this date have to be corrected in consequence. Figure 1 also shows the predictions of the differences between UTC and UTC(OP) made at the release of *Circular T*: in magenta, cyan and green, for *Circular T* 330, 331 and 332, respectively. The variation of the slope of the predictions is clearly visible for *Circular T* 330 and 332, and corresponds to the update of the monthly steering. This is less visible for *Circular T* 331 because the steering remained very close to that of *Circular T* 330. The error bars are empirically evaluated by considering 1 ns for the estimation of the time difference and 50 ps per day in frequency prediction, corresponding to an uncertainty of about 5×10^{-16} on the daily estimation of the frequency of the UTC(OP) generated signal. The uncertainty of the time link to UTC reported in *Circular T* ranges from 1.0 ns to 1.5 ns. By considering that one potential bias in the time link will not change from month to month by a noticeable amount, the chosen value of time uncertainty seems realistic. The frequency uncertainty is in principle a combination of the

uncertainty of the evaluation of the frequency averaged over one *Circular T* period and of the instability of both time scales UTC and UTC(OP) during the same period. The results presented in section 4 confirm the predictability of frequency at 5×10^{-16} over one month.

In implementing this algorithm, there is no reason why all the three components of the frequency corrections could not be applied by the same device. Therefore the frequency offset introduced by the frequency offset generator will simply be the sum of the FLL and PLL control signals evaluated each month and kept constant until the next *Circular T* publication, in addition to the daily correction computed by the feed-forward software.

3. UTC(OP) implementation

In October 2012 the new algorithm was implemented by using the frequency offset generator and the signal distribution system that were already in operation. Apart from the new data processing and the use of fountain data, the only change in the hardware setup was the replacement of the 5 MHz signal of the master Cs clock by the similar signal provided by the chosen H-maser. At the same period a new low noise hardware system operating at 100 MHz was developed and tested. It was fully characterized and the reliability was tested by operating in parallel with the old setup until June 2015, when it was declared operational. The different pieces of equipment using UTC(OP) signals were progressively connected to the new setup by keeping the two time scales in parallel operation. This allowed for a smooth transition almost transparent for all the equipment fed by the UTC(OP) signal. In November 2015 the old equipment was definitively removed from the operational system, and it is now used for scientific tests and additional redundancy.

A simplified synoptic diagram of the new generation chain of UTC(OP) is shown in figure 2. The ensemble of atomic fountains PSFS (FO1, FO2-Cs, FOM, and FO2-Rb) [7, 8] developed at LNE-SYRTE is reaching an accuracy between 2 and 6×10^{-16}. All the fountains share a common microwave local oscillator which is based on a cryogenic sapphire oscillator (CSO) [11], developed by the University of Western Australia, and phase locked to one of our four H-masers with a 1000 s time constant. Thus the fountains, taking benefit of the low noise of the CSO, are reaching the quantum projection noise limit [12]. On averaging periods longer than the time constant of the CSO PLL, the fountains measure the frequency of the H-maser. This system is in almost continuous operation since more than fifteen years [7, 8].

A software that is run automatically every hour corrects the raw cycle-by-cycle fountain data for all the fountain systematic shifts. The same software then produces the compact data files effectively used in generating UTC(OP) and in routine H-maser and fountain monitoring. The format of those files, that we call 'pack' files, was established more than ten years ago for local fountain frequency comparisons. By considering the noise of the fountains and of the local oscillators, it was decided to produce files containing a reduced number of
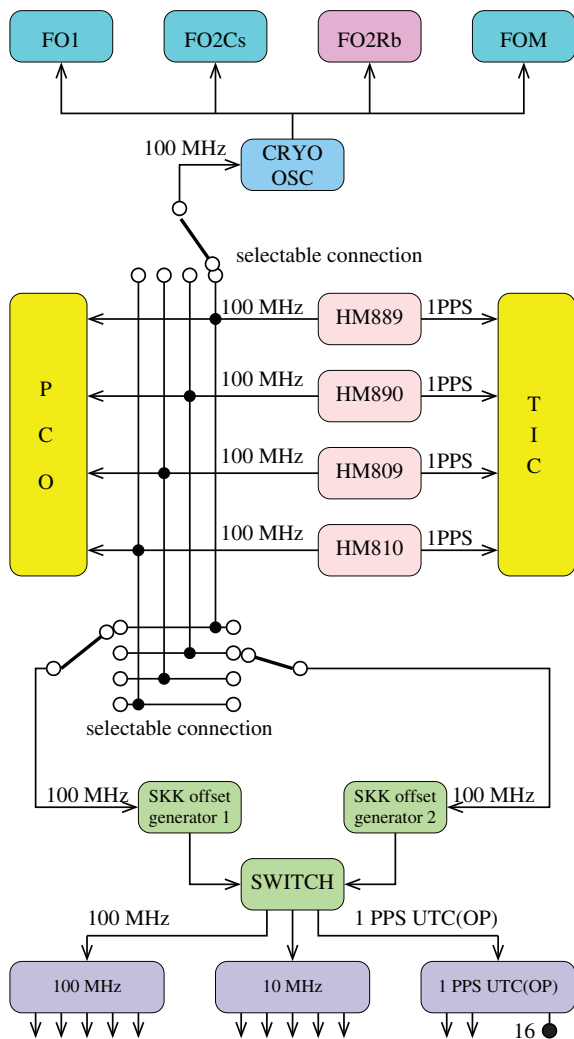
Figure 2. Simplified synoptic diagram of the equipment used for the realization of UTC(OP). PCO is a 100 MHz phase comparator, TIC is a time interval counter. The output labeled 16 of the 1 PPS distribution amplifier is the reference point for UTC(OP), defined at a trigger level of 1 V. The TIC reference is UTC(OP).

Figure 3. 100 MHz output phase noise spectral density of the frequency offset generator measured with a 5125A symmetricom analyzer, with an applied offset frequency of 2.1×10^{-12}.

Figure 4. Allan deviation of the noise floor of the frequency offset generator, with a 2.1×10^{-12} offset. A stability below 10^{-16} is reached for averaging periods longer than 2000 s.

points per day, the remaining useful data still being dominated by white frequency noise. The simple rule was to divide each day in 10 data sets covering the epochs from 0.0 d to 0.1 d, from 0.1 d to 0.2 d, etc. To deal with the drift of the local oscillator shared by the fountains, a linear fit is performed and outliers are removed by successive iterations. If at the end of the process there are enough valid points, the relative frequency at the center of the nominal interval is computed, labeled by the time-tag of the middle epoch of that interval. The data differences can then be computed over synchronous dates.

In addition, at regular intervals, the main data management system also retrieves the data from the ensemble of phase comparators (PCO) and from the time interval counters (TIC) measuring the delays between all the generated 1 pulse per second (1 PPS) signals. This allows for the quasi real time computation of the frequency of the four H-masers against all the fountains that are in nominal operation. Although it would be possible to take advantage of this ensemble by setting-up some data fusion process, we choose the simple option of
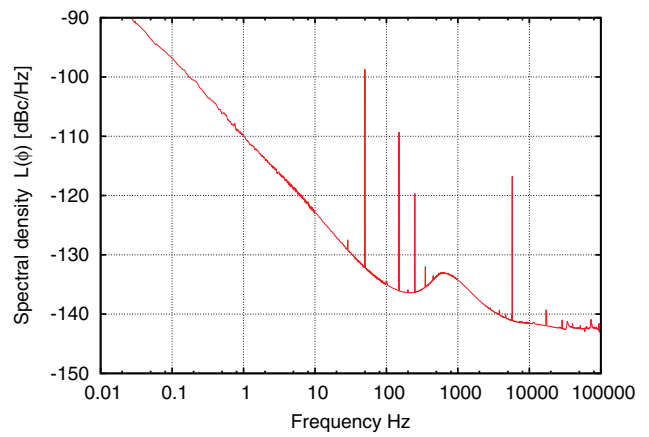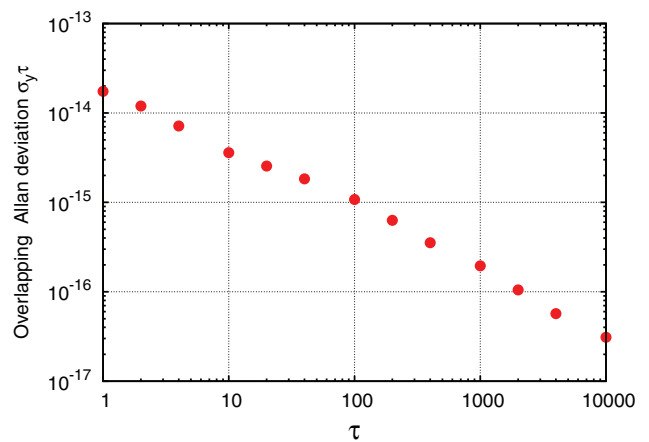
a software parameter which selects the fountain to be used for the generation of UTC(OP). It must be pointed out that, thanks to the availability of the computed frequency of all the H-masers, the H-maser selected as reference for the cryogenic oscillator is not necessarily the one used in the UTC(OP) generation.

In order to improve the short term stability of the time scale that was limited by the old 5 MHz device, a new kind of frequency offset generator specially designed to operate at 100 MHz was developed in collaboration with the SKK Electronics Company [13]. Figure 3 presents the phase noise and figure 4 the Allan deviation of such a device, measured by a Symmetricom 5125A analyzer, both for a frequency offset of 2.1×10^{-12}. We observe that the noise floor of the system is at least one order of magnitude lower than the noise of a H-maser. Two such devices have been built, allowing to produce two time scales using the 100 MHz output of two different H-masers feeding the two frequency offset generators.

In collaboration with the same company, a switch that allows for the hot swapping between the two time scales was also developed, with negligible effect on the phase and on the amplitude of all the UTC(OP) signals. In the old setup,
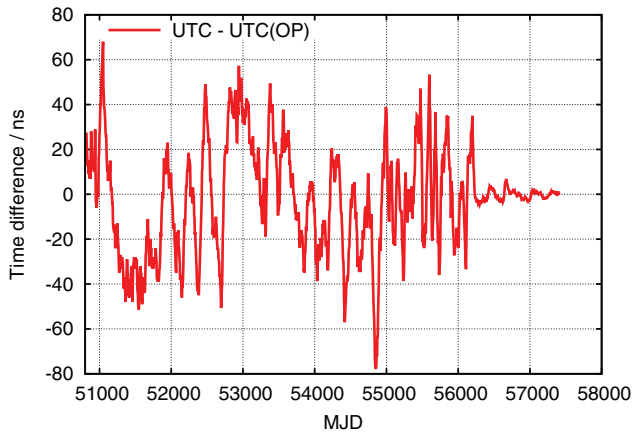
Figure 5. Time difference between UTC and UTC(OP) since 1998. The upgrade of UTC(OP) occurred at MJD 56229.

Figure 6. Time differences between UTC and three fountain based UTC(k) since the implementation of the new algorithm in UTC(OP).

like in many laboratories, there was a backup system running to generate a parallel time scale, allowing the possibility of changing the input of the signal distribution in case of a failure of the main signal generation chain. The major drawback of such a traditional setup is the fact that if a swapping is necessary, there is an interruption of the signal, also producing new delays to be evaluated, and possible signal amplitude variations. This kind of operation had to be planned well in advance in agreement with users requirements. The new device developed to solve this issue has two 100 MHz signal inputs, fed by the two time scales and provides three coherent outputs at 100 MHz, 10 MHz and 1 PPS, that feed the UTC(OP) signal distribution. This switch not only allows for the commutation between inputs but can also be used to monitor the phase difference between the two 100 MHz input timescales with a sub-ps resolution. This makes possible the fine adjustment at the ps level of the phase between nominal and alternate time scales, and the commutation can be carried out with an undetectable phase step on the output signal. An example of commutation in operational conditions is presented in section 4.3.

The development of a software for automatic fault detection and H-maser replacement is under consideration, but more operational experience with the present setup is first required. We believe that the careful observation of all the parameters by an operator allows for preventive maintenance. The occurrence of a sudden unpredictable fault is very uncommon and we prefer to take this risk instead of having a too complicated software that could go out of control.

At the installation of the new hardware the reference point of UTC(OP), that was previously defined at the input of a TIC, was changed. It is now based on the 1 PPS signal available on connector 16 of the main PDU loaded by a 50 Ω impedance. The time marker occurs when the rising edge of the 1 PPS reaches the level of 1 V. With this new definition the accuracy of a delay measurement against the reference point is not limited by the behavior of the input channel of a TIC.

Since the first implementation in October 2012, only a minor change was introduced in the algorithm, in order to take into account the fact that the first points published in the *Circular T* are obtained with the coefficient of the former
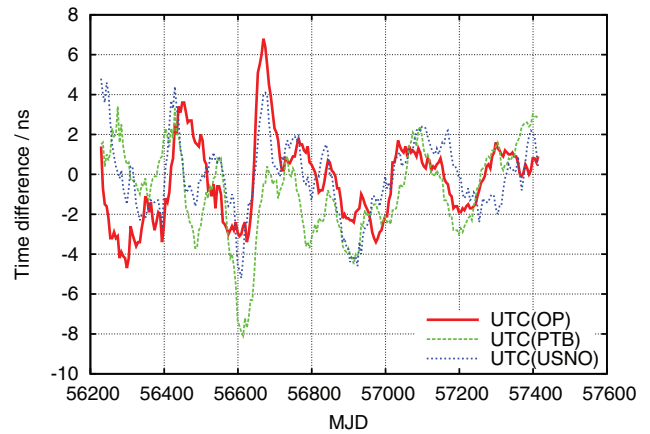
month, as described in section 2. At the beginning, the software implementing the FLL and the PLL for the steering of UTC(OP) to UTC consisted of several successive tasks manually launched. Today, a single script is launched manually when the *Circular T* shows up on the BIPM website. The software evaluates daily the frequency of all the H-masers against all the operational fountains and generates the output commands to drive the two 100 MHz frequency offset generator for the operational and alternate time scales, as well as to drive the two old 5 MHz frequency offset generators used for scientific purposes and additional redundancy. When necessary, a parameter configuration file can be modified in order to change the reference fountain, or the reference H-maser dedicated to each time scale, or whatever else.

4. UTC(OP) performances

4.1. Time domain characterization

Figure 5 shows the improvement by more than one order of magnitude of the new UTC(OP) as compared to the previous system based on a commercial thermal beam cesium clock. As mentioned in section 2 the ultimate goal of UTC(OP) is the real time realization of UTC with the best approximation. The indicator that better illustrates the obtained result is in this case simply the time difference between UTC and UTC(OP). This difference, since the implementation of the new algorithm in October 2012, is reported in figure 6 together with the time difference between UTC and two other UTC(k) also exploiting atomic fountains [14, 15]. Over the last three years UTC(OP) remained close to UTC to well below 10 ns, with an average difference of 0.33 ns and a standard deviation of 2.1 ns. The difference is less than 5 ns if we except a short period around MJD 56650. However, we note that the two other UTC–UTC(k) comparisons, that present equivalent performances, also exhibit the same feature around MJD 56650. Over the year 2015, the difference between UTC(OP) and UTC remained even below 2 ns. It should be noted that this level of performances approaches the uncertainty of the time transfer links.
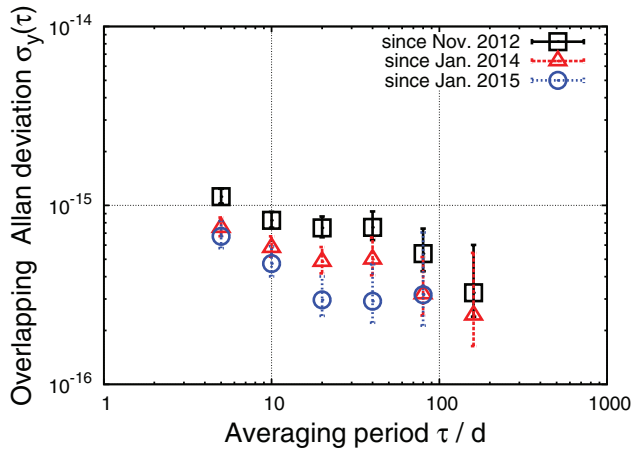
Figure 7. Relative frequency stability of UTC–UTC(OP): black squares are computed by taking into account all data since November 2012, red triangles by taking the data since January 2014, while blue circles represent the stability during 2015.
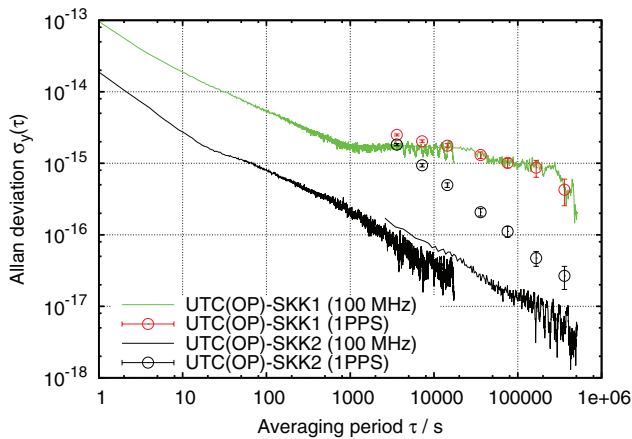

Figure 8. Relative frequency instability of UTC(OP) against the alternate time scale SKK1 (green and red). Residual noise of the measurement system, computed against the active frequency offset generator SKK2 (black). The comparisons at 100 MHz are carried out by using a PCO. The 1 PPS measurements are made by a SR620 TIC.

4.2. Frequency domain characterization

The relative frequency instability of UTC–UTC(OP) is shown in figure 7. The squares represent the Allan deviation computed by taking into account all the data available after the implementation of the new algorithm. The triangles show the Allan deviation since January 2014 (MJD 56659), when a new clock weighting procedure was introduced in the UTC computation [16]. The circles show the Allan deviation during calendar year 2015. The stability at 5 d is at the level of 10^{-15} or lower. It reaches 2–3×10^{-16} for averaging periods of 100 d thanks to the steering to UTC. Although there is no identified event explaining the improvement observed in 2015, we believe that this might be the result of the progressive improvement of the UTC(OP) hardware setup, less sensitive today to temperature fluctuations, and to an improved signal distribution. Figure 8 presents the statistical analysis (ADEV) of the comparisons of UTC(OP) to two outputs, of SKK1 and SKK2, as measured by a 100 MHz PCO (continuous lines) and

by the TIC used for hourly measurements (circles) over the period MJD 57375-57404. For the stability analysis we have plotted two curves: one relative to data covering the overall period averaged over 0.01 d to get the long term stability, another one over a given day inside the interval to analyze the short term stability. During the period analyzed, UTC(OP) was based on SKK2 referenced to H-maser 810. The green and red (upper) curves present the comparison between SKK1 using H-maser 889 and UTC(OP). On the short term, they correspond to the noise of the comparison between the two H-masers which varies between 1×10^{-13} at 1 s and 1×10^{-15} at 1 d. On longer averaging periods, the stability reaches the 1×10^{-16} level thanks to the daily steering by the fountains that removes the frequency drift of both H-masers. In the black lines, the noise of the H-maser and of the frequency offset generator is removed because it is in common mode. The stability varies from 2×10^{-14} at 1 s down to the 10^{-17} range after a 1 d averaging period. The circles correspond to the noise of the TIC which reaches the 1×10^{-16} level after 1 d of averaging time. This confirms that the noise of the frequency offset generator is negligible as compared to the noise of an H-maser exhibiting a good short term stability. These results are at the limit of the noise floor of the PCO and have been confirmed by using a Symmetricom 5125A signal analyzer (see figures 3 and 4). This demonstrates that the new hardware developed for the generation of UTC(OP) is presenting a noise floor improved by about one order of magnitude over all averaging periods. We note also that the H-masers and the PCO are located inside the clock room in the basement of the building, whereas the UTC(OP) generation and distribution system are located two floors above. Thus this measurement also validates the cable installation to better than 1×10^{-17}. One of the motivations to develop the new hardware and to improve the signal distribution was also the space mission Atomic Clock Ensemble in Space (ACES) [17]. The obtained results are fully compatible with the specifications of the ground terminal of the microwave link. To provide the reference to this equipment, to be installed on the roof of a building at OP, we plan to send one of the 100 MHz signals via a 1 GHz compensated fiber link.

4.3. Commutation of the switch

Figure 9 shows the performance of the new system implemented to generate UTC(OP) in a real case of swapping between the nominal (H-maser 889 steered by SKK1) and alternate (H-maser 810 steered by SKK2) timescales. Because the H-maser 889 presented a failure in the parameter monitoring board, we decided to switch UTC(OP) generation from SKK1 to SKK2, on MJD 57364, in order to allow for the replacement of the faulty electronic card. Just before the switch, the alternate time scale was manually aligned to UTC(OP) to a few ps by applying a 200 ps time step, based on the reading of the phase comparator of the switch. Then the command to change the reference input was sent to the switch. After repair, the H-maser 889 was restarted, and the SKK1 time scale was manually aligned to UTC(OP) again. The excursion of more than 1 ns which
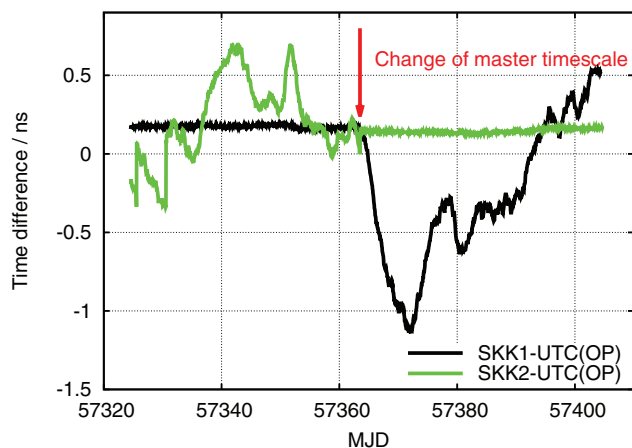
Figure 9. Time differences between UTC(OP) and the two timescales SKK1 and SKK2 measured by the main data acquisition system. Until MJD 57364 SKK1 is the UTC(OP) source, while SKK2 is used as an alternate time scale. After MJD 57364 the roles of the two time scales are interchanged.

can be seen in figure 9 is probably due to a change in the frequency of the H-maser 889 as a consequence of the two hours shut down. After a few days of automatic frequency steering, the difference between operational and alternate time scales was reduced to less than 1 ns, allowing for a switch back to H-maser 889 if required. Figure 9 also shows the performances that can be obtained with two times-cales based on two different H-masers. Even though these H-masers are well predictable, we observe fluctuations of about 1 ns that are due to their own behavior.

5. Conclusion

We have presented the new algorithm implemented for the generation of UTC(OP). It is based on a feed-forward control allowing to compensate daily the frequency of a H-maser as measured by the SYRTE atomic fountains. An additional fine steering based on the sum of a FLL and a PLL using *Circular T* data is updated monthly to maintain UTC(OP) close to UTC.

The new algorithm was implemented in October 2012 using the old hardware operating at 5 MHz. All the equipment was then progressively replaced by a new one, part of which designed on purpose. The transition phase is now finished and UTC(OP) is currently the unique signal distributed to all time transfer equipment and to time users. All relevant interme-diate signals have been characterized, as well as the UTC(OP) signals at 100 MHz, 10 MHz and 1 PPS. The measured fre-quency stability confirms that the UTC(OP) 100 MHz signal is ready to feed the ground terminal of the ACES microwave link. The UTC(OP) noise is an exact replica of the H-maser noise for periods shorter than a few days, but it is much better than an H-maser for longer periods, following the long term stability of the laboratory atomic fountains.

Over the first three years of operation, benefiting from the almost continuous operation of the LNE-SYRTE atomic foun-tains, UTC(OP) was one of the best real time realization of UTC remaining well below 10 ns close to UTC. Throughout

the year 2015 the time deviation of UTC(OP) from UTC stayed below 2 ns. These performances are reaching the uncertainty of the operational time transfer techniques, that are currently the limiting factor for UTC(k) time scales.

Disclaimer

Product names and model numbers of the equipment are included for reference only. Neither endorsement nor criti-cism is implied.

Acknowledgments

References

[1] Quinn T J 1994 News from the BIPM *Metrologia* **31** 55
[2] Uhrich P, Valat D, Brunet M, Marechal J, Beltan T and Suard N 2005 The French time reference UTC(OP), and the connection of the EGNOS network time *19th European Frequency and Time Forum* pp 643–8
[3] Parker T and Levine J 1997 Impact of new high stability frequency standards on the performance of the NIST AT1 time scale *IEEE Trans. Ultrason. Ferroelectr. Freq. Control* **44** 1239–44
[4] Clairon A, Ghezali S, Santarelli G, Laurent P, Lea S, Bahoura M, Simon E, Weyers S and Szymaniec K 1996 Preliminary accuracy evaluation of a cesium fountain frequency standard *Proc. of 5th Symp. on Frequency Standards and Metrology* ed J Bergquist (Singapore: World Scientific)
[5] Bize S, Sortais Y, Santos M, Mandache C, Clairon A and Salomon C 1999 High-accuracy measurement of the ^{87}Rb ground-state hyperfine splitting in an atomic fountain *Europhys. Lett.* **45** 558
[6] Guéna J, Rosenbusch P, Laurent P, Abgrall M, Rovera D, Santarelli G, Tobar M, Bize S and Clairon A 2010 Demonstration of a dual alkali Rb/Cs fountain clock *IEEE Trans. Ultrason. Ferroelectr. Freq. Control* **57** 647–53
[7] Guéna J *et al* 2012 Progress in atomic fountains at LNE-SYRTE *IEEE Trans. Ultrason. Ferroelectr. Freq. Control* **59** 391–409
[8] Guéna J, Abgrall M, Clairon A and Bize S 2014 Contributing to TAI with a secondary representation of the SI second *Metrologia* **51** 108
[9] Rovera D 2012 Aplicações metrológicas de um pente de frequências *Technical Report* CNPq:551404/2011-6 INMETRO in Portuguese
[10] Franklin G F, Powell J D and Emami-Naeini A 1986 *Feedback Control of Dynamic Systems* (Reading, MA: Addison-Wesley)
[11] Mann A G 2000 Ultrastable cryogenic microwave oscillators *Frequency Measurement and Control* (*Topics in Applied Physics* vol 79) ed A Luiten (Berlin: Springer) pp 37–67

[12] Santarelli G, Laurent Ph, Lemonde P, Clairon A, Mann A G, Chang S, Luiten A N and Salomon C 1999 Quantum projection noise in an atomic fountain: a high stability cesium frequency standard *Phys. Rev. Lett.* **82** 4619

[13] Rovera G, Abgrall M and Siccardi M 2012 Characterization of an auxiliary offset generator for steering of H Masers *26th European Frequency and Time Forum* pp 14–5

[14] Bauch A, Weyers S, Piester D, Staliuniene E and Yang W 2012 Generation of UTC(PTB) as a fountain-clock based time scale *Metrologia* **49** 180

[15] Peil S, Hanssen J L, Swanson T B, Taylor J and Ekstrom C R 2014 Evaluation of long term performance of continuously running atomic fountains *Metrologia* **51** 263

[16] Panfilo G, Harmegnies A and Tisserand L 2014 A new weighting procedure for UTC *Metrologia* **51** 285

[17] Salomon C, Cacciapuoti L and Dimarq N 2007 Atomic clock ensemble in space: an update *Int. J. Mod. Phys.* D **16** 2511–23